Fully Automatic Organ Localization in Medical Images Using Improved Random Regression Forests

Prasad Samarakoon, Emmanuel Promayon and Céline Fouard
TIMC-IMAG Laboratory, CNRS UMR 5525 , University of Joseph Fourier, Grenoble, France
{*Prasad.Samarakoon, Emmanuel.Promayon, Celine.Fouard*} *@imag.fr*

***Index Terms*—localization, random regression forests, medical image analysis**

The article presents the use of an improved random regression forest method to localize multiple organs in Computed Tomography (CT) images. The method was trained using 50 CT images and tested on 25 CT images yielding 15.66% improvement on the localization with respect to the bounding wall prediction error compared to the state of the art results.

I. Introduction

RANDOM Regression Forests (RRF) were first used in the field of medical image analysis by Criminisi et al.[1] to automatically localize multiple organs in CT images. The organ localization problem was solved as a continuous parameterization regression problem in which the image voxels were directly mapped to a localized organ bounding box.

II. Methodology

RRF consists of a collection of Random Regression Trees (RRT). Each RRT comprises of split and leaf nodes (Figure 1). At each split node j the following binary split function (whose sole purpose is binarily dividing the incoming voxels) is defined:

$$\xi_j > f\left(\mathbf{v}, \theta_j\right) > \tau_j \tag{1}$$

where $\xi_j, \tau_j \in \mathbb{R}$ are upper and lower thresholds and $f\left(\mathbf{v}; \theta_j\right)$ is the weak learner response computed at the voxel $\mathbf{v}$ and θ_j is the weak learner (inspired by [1], [2], [3]). Each leaf node (l) predicts the a posteriori probability of an organ's bounding box with respect to the position of the leaf:

$$\Pr\left(\mathbf{d}_c|l\right) = \mathcal{N}\left(\mathbf{d}_c, \bar{\mathbf{d}}_c, \Lambda\right) \tag{2}$$

where $\mathbf{d}_c$ is the bounding box vector of organ C; $\bar{\mathbf{d}}_c$,$\Lambda$are mean and covariance of $\mathbf{d}_c$.

RRF has two main phases. 01.) Training phase: building RRF using training images where the target organ's bounding boxes are manually delineated. 02.) Testing phase: using the trained RRF on a new image to predict the localization of target organs.

At the training phase each split node is given a collection of different split configurations consisting of a lower and upper threshold and a weak learner. The split function is applied to all voxels reaching that particular split node across all available split configurations. Then the split configuration that best discriminates the incoming voxels is found using an information gain measure (Eq. 3). The lower and upper thresholds and weak learner of the selected split configuration are saved as the values of the corresponding split node.

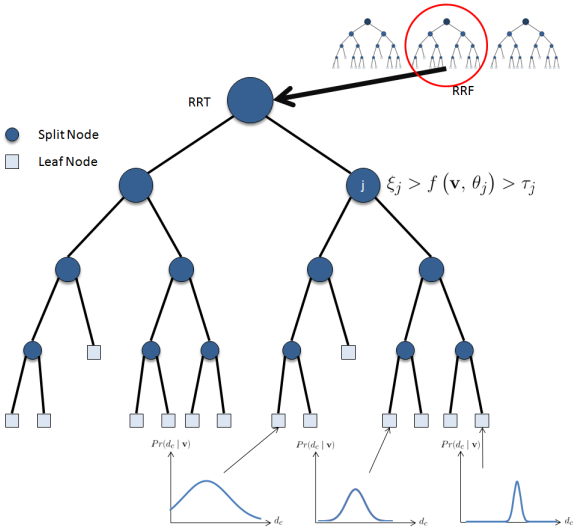

Figure 1. **Random Regression Forest** is a collection of regression trees. Each regression tree consists of split nodes (including root) and leaf nodes. Split nodes have the responsibility of dividing the incoming voxels into two parts depending on the response of the split function. Ultimately, the leaf nodes define the a posteriori probabilities of the organ bounding boxes with respect to the position of the leaf.

$$IG(\mathcal{S}, \theta) = H(\mathcal{S}) - \sum_{i=\{L,R\}} w_i H(\mathcal{S}_i) \tag{3}$$

where *H*: entropy; $\mathcal{S}$: set of voxels reaching the split node; *L,R*: left and right children resulted from the parameters defined by ξ_j, τ_j, θ_j and $\omega_i = \frac{\mathcal{S}_i}{\mathcal{S}}$: the relative portion of voxels reaching the child. Eq. 3 can be approximated by:

$$IG(\mathcal{S}, \theta) = \log\left(|\Gamma\left(\mathcal{S}\right)|\right) - \sum_{i=\{L,R\}} w_i \log\left(|\Gamma\left(\mathcal{S}_i\right)|\right) \tag{4}$$

where $\Gamma\left(\mathcal{S}\right)$: $\Gamma = \mathrm{diag}\left(\Lambda_{ld}, \Lambda_{rd}\right)$.

Growing of RRT is stopped when the depth of RRT has reached a predefined maximum decision level or when the

number of voxels reaching the node is below a certain predefined threshold or when there is no positive information gain. Leaf nodes of a trained RRT will store $\bar{\mathbf{d}}_c$ and Λ_c of $\mathbf{d}_c$s of all the voxels aggregated at the particular leaf. Hence at leaf nodes, $\Pr(\mathbf{d}_c|l)$ is known.

At the testing phase, every voxel $\mathbf{v}$ of an unseen image volume $\mathcal{V}$, is pushed through each RRT where the split function is applied at each split node and is eventually aggregated at a leaf node per RRT of RRF. Once all the voxels are treated, the absolute position of each leaf node $\hat{\mathbf{v}}$ is found by calculating the mean of all voxels aggregated at that leaf node contrary to using the mode as in [1] and [4].

Then absolute position of the bounding box vector $\Pr(\bar{\mathbf{b}}_c|l)$ can be known since $\mathbf{b}_c = \hat{\mathbf{v}} - \mathbf{d}_c$. Finally, the absolute position of the organ's bounding box ($\mathbf{b}_c$) is found by taking the total probability summation:

$$\Pr(\mathbf{b}_c) = \sum_{t=0}^{T} \sum_{l \in \mathcal{L}_t} \Pr(\mathbf{b}_c|l) \Pr(l) \tag{5}$$

where $\mathcal{L}_t$: subset of leaf nodes used for calculation; $\Pr(l)$: proportion of voxels at leaf l with respect to all voxels of $\mathcal{L}_t$. $\mathcal{L}_t$ is determined by choosing the best discriminating leaf nodes of RRF having the highest confidence in their predictions.

III. Results and Discussion

RRF method was implemented to localize left and right kidneys of 75 CT images belonging to 75 patients randomly selected from the CHU Grenoble database without considering any specific pathology. From which, 50 and 25 images were randomly selected for training and testing respectively. RRF consisted of 3 RRTs using 9 maximum decision levels (parameters were influenced by [1]). Results were produced within 1.62 seconds on average for an image of average size of 30 cm x 30 cm x 40 cm (100 x 100 x 245 voxels).[1]

Our method produced better results in comparison to the literature with respect to the bounding wall prediction error BWPE[2] (Table Ia) and centroid hit error CHE[3] (Table Ib). The use of a predictive determination of Lt using the input image instead of a hardcorded percentage of voxels (1% in [1] and 75% in [4]) contributes to the amelioration. In addition, using mean instead of mode when calculating the leaf node position seems to better preserves the probabilistic impact and to counter some ill effects of the outliers.

[1]Results were generated on an Intel® Xeon® @ 3.00 GHz machine with 32 GB of RAM using sequential programming.

[2]BWPE is the absolute error between the automatically predicted bounding box wall and the manually segmented bounding box wall [5].

[3]CHE occurs when the centroid of the automatically predicted bounding box falls outside the bounding box drawn manually [5]. In the case of a CHE, it is further investigated in which direction/directions the Centroid has overflown with respect to the manually drawn bounding box. In 3D image volumes, three directions; namely, left to right, anterior to posterior and feet to head are present.

	Our Method			*Criminisi [4]*			*Pathak[5]*		
	M	Sd	Md	M	Sd	Md	M	Sd	Md
RK	13.2	12.2	10.3	16.1	15.5	-	18.5	18.0	12.3
LK	11.9	11.9	9.2	13.6	12.5	-	17.3	16.5	12.8

(a)

	Our Method		*Pathak [5]*	
Direction	RK	LK	RK	LK
All	8%	8%	26%	20%
Left to right	0%	0%	8%	10%
Anterior to posterior	0%	4%	10%	12%
Inferior to superior	8%	4%	22%	16%

(b)

Table I. **(a) Bounding wall prediction error comparison with *Criminisi et al.* [1], [4] and *Pathak et al.* [5]** in mm**.** RK, LK: Right and left kidney, M: mean, Sd: standard deviation, Md: median. **(b) Centroid-hit error comparison with *Pathak et al.*** [5] (where 100 testing images were used).

IV. Conclusion

Random Regression Forests method with the intuitive testing mechanisms proposed is quite efficient in localizing organs fully automatically producing results within 1.62 seconds. With the proposed improvements, mean BWPE was reduced by 15.66% with respect to the previous state of the art results.

Our future work will focus on reducing the training time by using parallel programming and applying RRF to other image modalities such as MRI.

Acknowledgements: This work was supported by the French ANR within TECS project Robacus (ANR-11-TECS-020-01) and within the Investissements d'Avenir programme - Labex CAMI (ANR-11-LABX-0004). The authors are grateful to Prof. Ivan Bricault of CHU Grenoble for providing the CT images.

References

[1] A. Criminisi, J. Shotton, D. Robertson, and E. Konukoglu, "Regression forests for efficient anatomy detection and localization in CT studies," in *Medical Computer Vision. Recognition Techniques and Applications in Medical Imaging*, no. 6533 in Lecture Notes in Computer Science, pp. 106–117, Springer Berlin Heidelberg, Jan. 2011.

[2] A. Criminisi, J. Shotton, and S. Bucciarelli, "Decision forests with long-range spatial context for organ localization in CT volumes," in *MICCAI Workshop on Probabilistic Models for Medical Image Analysis*, 2009.

[3] R. Cuingnet, R. Prevost, D. Lesage, L. D. Cohen, B. Mory, and R. Ardon, "Automatic detection and segmentation of kidneys in 3D CT images using random forests," in *Medical Image Computing and Computer Assisted Intervention MICCAI 2012*, no. 7512 in Lecture Notes in Computer Science, pp. 66–74, Springer Berlin Heidelberg, Jan. 2012.

[4] A. Criminisi, D. Robertson, E. Konukoglu, J. Shotton, S. Pathak, S. White, and K. Siddiqui, "Regression forests for efficient anatomy detection and localization in computed tomography scans," *Medical Image Analysis*, vol. 17, no. 8, pp. 1293–1303, 2013.

[5] S. D. Pathak, A. Criminisi, J. Shotton, S. White, D. Robertson, B. Sparks, I. Munasinghe, and K. Siddiqui, "Validating automatic semantic annotation of anatomy in DICOM CT images," in *SPIE Medical Imaging 2011: Advanced PACS-based Imaging Informatics and Therapeutic Applications*, vol. 7967, pp. 796704–796704, Mar. 2011.